

# ECE 445

## Insole for Gait Monitoring and Fall Risk Research in Older Adults

---

By

Lily Hyatt

Nasym Kushner

Jessica Sun

Final Report for for ECE 445, Senior Design, Spring 2025

TA: Kaiwen Cao

Professor: Michael Oelze

07 May 2025

Project No. 48

## Abstract

This project presents the design and implementation of a preventative fall-risk monitoring system that integrates a triboelectric nanogenerator (TENG) sensor developed by Professor Manuel Hernandez and his lab into a wearable device. The sensor generates voltage proportional to foot pressure while walking, enabling real-time gait analysis. The device, which is worn on both feet, synchronizes step data and transmits measurements via Bluetooth Low Energy (BLE) to a mobile app. The system integrates a custom PCB featuring power regulation, signal conditioning, an ADC, and an ESP32-S3 microcontroller running step-detection firmware. To ensure accurate analog-to-digital conversion, the analog front-end scales and buffers the signal output from the sensors, which addresses high-voltage and low-current challenges. The mobile app allows users to track gait metrics and device status in real time. This wearable device is a step toward proactive fall prevention through real-time monitoring of gait-related risk factors.

## Contents

<b>1. Introduction</b>	<b>3</b>
1.1 Problem	3
1.2 Solution	3
1.3 High-Level Requirements	3
<b>2. Design</b>	<b>4</b>
2.1 Block Diagram	4
2.2 Power Subsystem	5
2.3 Measurement Subsystem	7
2.4 Data Processing Subsystem	10
2.5 Programming Subsystem	13
2.6 Mobile Application	14
2.7 Mechanical Design	16
<b>3 Cost and Schedule</b>	<b>17</b>
3.1 Costs	17
3.2 Schedule	18
<b>3 Conclusion</b>	<b>20</b>
3.1 Safety and Ethics	20
<b>4 Appendix A Costs</b>	<b>22</b>
<b>5 References</b>	<b>25</b>

# 1. Introduction

## 1.1 Problem

Falls are a leading cause of injury among the elderly, with eight million adults over 65 suffering fall-related injuries each year. Of these, approximately three million require emergency medical care. In the U.S. alone, falls account for an average of 32,000 deaths annually, and globally, they are the second most common cause of unintentional fatalities [1]. Currently, the market offers only solutions that detect falls after they occur. Despite the evident need for preventative technology, existing smart home fall detection systems for high-risk individuals are insufficient, as they fail to incorporate real-time monitoring of fall risk factors and frailty progression.

## 1.2 Solution

To address this gap in the market, Dr. Manuel Hernandez's lab developed a triboelectric nanogenerator (TENG) sensor designed to be embedded in a shoe insole. This sensor generates a voltage proportional to the pressure applied when a person walks [2]. Our goal is to integrate this sensor into a wearable device that tracks gait patterns for data collection. Gait, which is the manner in which a person walks, provides key indicators of fall risk, such as poor balance and slow walking speed. The device will be worn on both feet, allowing us to measure step timing and synchronize data from both sensors. The collected information will be transmitted via Bluetooth to a mobile app, where users can view their gait analysis.

## 1.3 High-Level Requirements

1. The system must accurately measure the timing between steps with no more than one malfunction or error occurring per 1,000 steps.
2. The system must be able to synchronize two sensors in order to collect data from both feet while walking. The two sensors should be synchronized to an error margin of no more than 12ms.
3. The output voltage of the sensor must be stepped down by a factor of  $10/43 \pm 10\%$  to ensure that the signal can be clearly sent through the ADC without voltage clipping to be interpreted by the microcontroller.

## 2. Design

### 2.1 Block Diagram

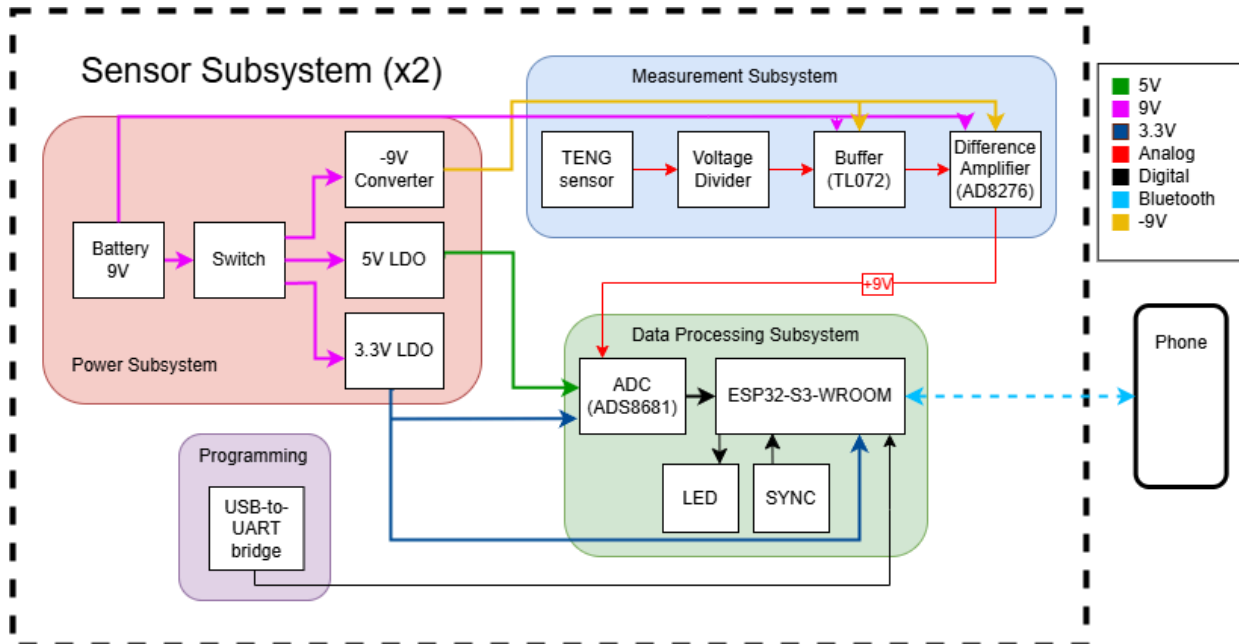


Figure 1: High-Level Block Diagram

Two identical PCBs—one per foot—integrate four subsystems (power, measurement, data processing, programming) and interface with a mobile app via Bluetooth LE. The power subsystem uses a switchable 9 V battery feeding a 5 V LDO for ADC analog inputs, a 3.3 V LDO for ADC digital domain and the ESP32-S3, and a -9 V converter to bias the TL072 buffer and AD8276 differential amplifier. The measurement subsystem scales the TENG sensor output via a resistor divider, buffers it with a TL072, then amplifies it with an AD8276 to  $\pm 5$  V for digitization. The data processing subsystem employs an ADS8681 ADC over SPI and an ESP32-S3-WROOM running step-detection firmware, drives a single status LED for user feedback, and uses a wired SYNC line—with a pushbutton—to link both PCBs and start their timers simultaneously, while streaming processed data over BLE. The programming subsystem provides a mini-USB-to-UART bridge to the ESP32's TX/RX pins for in-circuit firmware updates only.

## 2.2 Power Subsystem

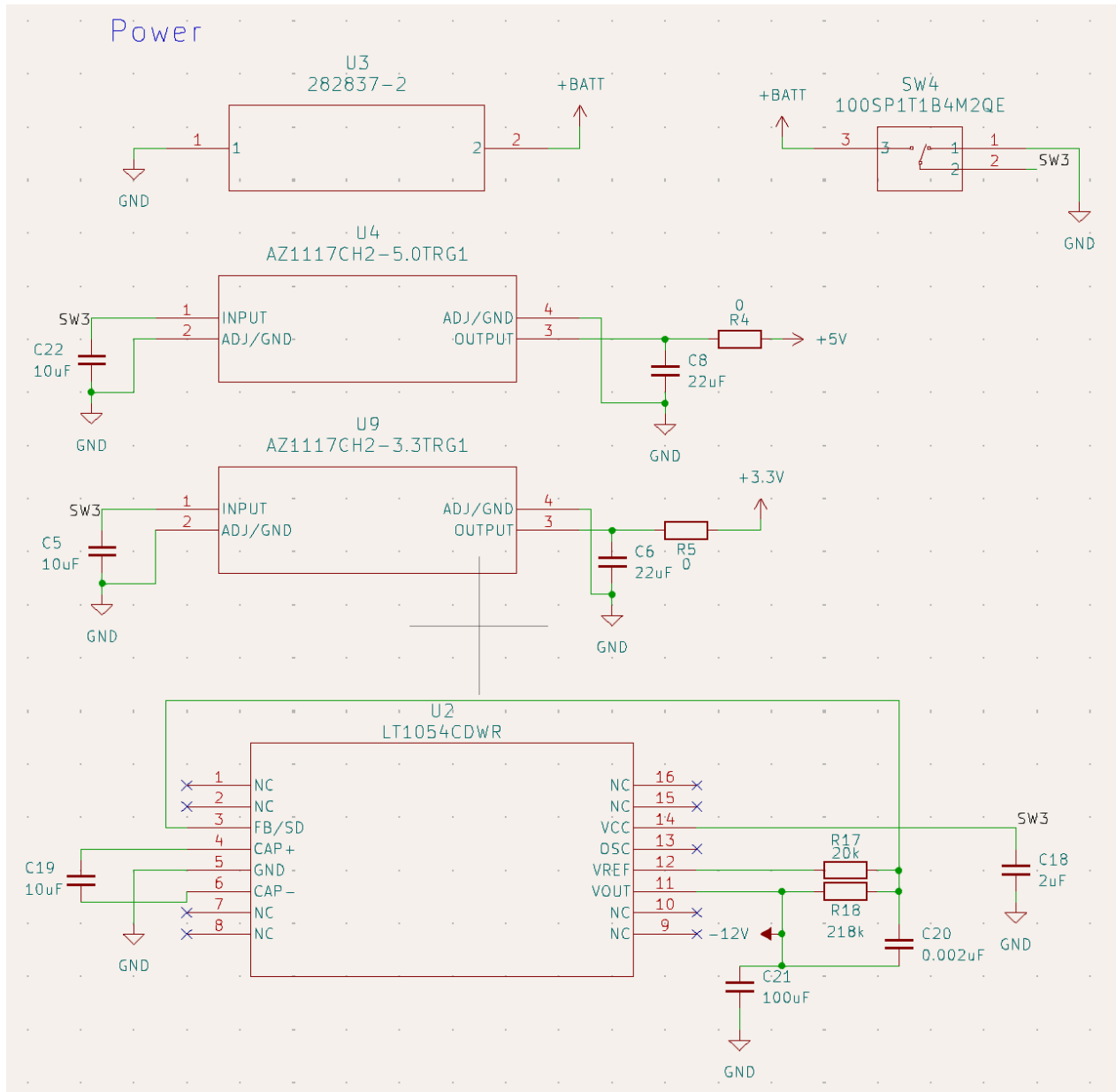


Figure 2: Schematic of power subsystem

The power subsystem for each foot-mounted PCB generates three regulated rails—+5 V, +3.3 V, and  $\pm 9$  V—from a user-switched battery and delivers them with low noise and adequate current headroom. The +5V LDO provides power to the analog input of the ADC. The +3.3V LDO provides power to the digital input of the ADC as well as the microcontroller (ESP32-S3-WROOM-1). The +9V from the battery and the -9V from the voltage converter are used to bias the difference amplifier that transforms the differential voltage from the sensor into a single-ended voltage signal. Originally, a 4V battery was used, but it could not satisfy the dropout requirements of the LDOs or the -9 V inverter. We were also using  $\pm 5$ V to bias the difference amplifier, and we also noticed that the output of the difference amplifier clipped at the bias voltage. The TENG sensor outputs a voltage greater

than 5V, but we wanted to capture the full signal. So, we switched to a +9V battery and used this to bias the amplifier. A switch allows the user to easily turn the device on and off.

The voltage converter (LT1054) outputs negative voltage proportional to the input voltage. We apply this component in its basic regulator configuration that allows us to choose resistor values to obtain the output voltage we need, which is -9V. We used the following equation to find the corresponding resistor value:

$$R_2 = R_1 \left( \frac{|V_{out}|}{\frac{V_{REF}}{2} - 40mV} + 1 \right)$$

where  $R_1=20k\Omega$ ,  $V_{out}=-9V$ , and  $V_{REF}=2.5V$ , we found  $R_2$  to be  $\sim 169k\Omega$ .

Table 1: R&V table for the power subsystem

Requirement	Verification	Result
The voltage converter should output a voltage in the range -8.8V to -9.2V to bias the differential amplifier, which takes a maximum $\pm 18$ supply voltage. In addition, the minimum and maximum input voltages of the difference amplifier are $-V_s+40$ and $V_s-40$ , respectively, and assuming $V_s=9V$ , the range is -35V to 35V, which is large enough to handle the output from the voltage divider.	Use a multimeter to probe the output of the converter and ground to ensure the voltage is within the specified range.	-8.971V
The +5V regulator must output a voltage that is within the range of input voltage of the ADC analog supply voltage, which is 4.75V to 5.25V.	Use a multimeter to probe the output of the LDO and ground to ensure the voltage is within the specified range.	5.012V
The +3.3V regulator must output a voltage that is within the range of input voltage of the microcontroller and ADC digital supply voltage. The ESP32-S3-WROOM-1 microcontroller has input voltage from 3V to 3.6V, and the ADC digital supply pin has a wider tolerance and can handle an input from 1.65V to the voltage on the analog supply pin, which is around 5V.	Use a multimeter to probe the output of the LDO and ground to ensure the voltage is within the specified range.	3.309V

## 2.3 Measurement Subsystem

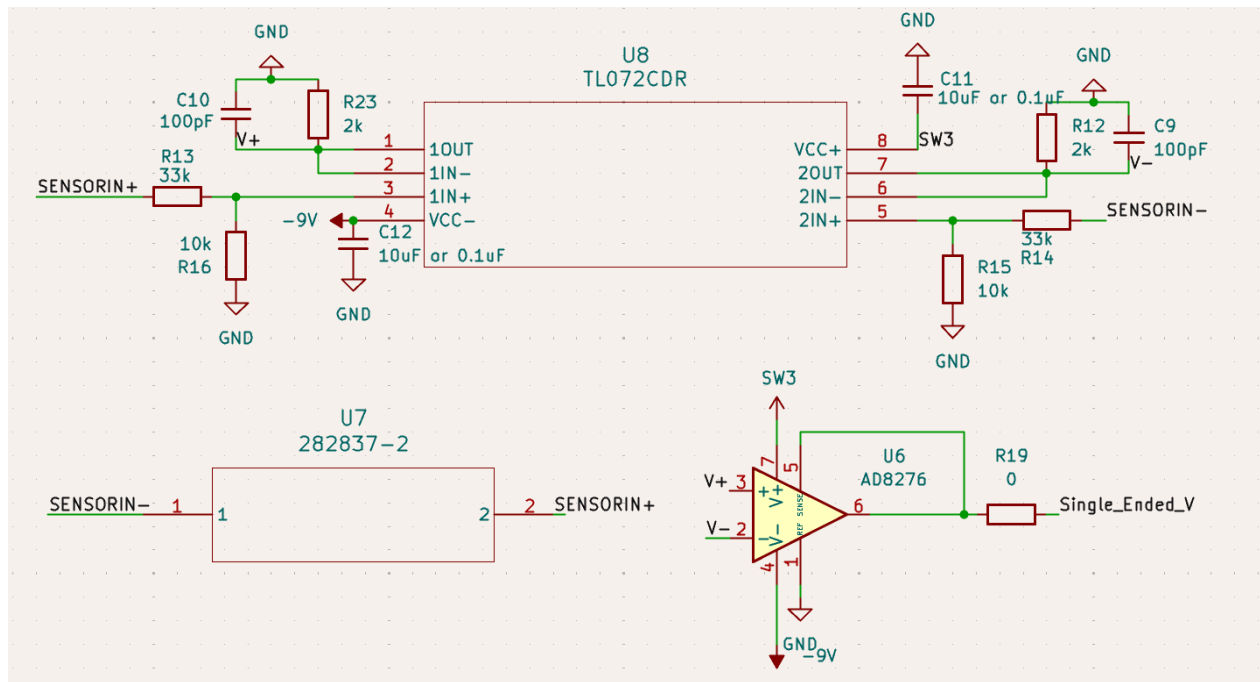


Figure 3: Schematic of the measurement subsystem

The measurement subsystem interfaces the TENG sensor and properly modifies the input signal to become compatible with the ADC for data processing. It is composed of the TENG sensor, voltage divider, unity gain low-current input op-amp, and unity gain difference amplifier.

The TENG sensor is made up of four layers (a conductive fabric top electrode; a carbonized orange-peel (COP)/PDMS positive layer; a microstructured PDMS negative layer; and a COP/PDMS conductive bottom electrode, all encapsulated in PDMS). This full sensor composition is shown in Figure 4. Under gait loading (1–5 Hz, 10 N), this sensor produces up to 40 V. This limit was confirmed in our own testing under human loading conditions [2].

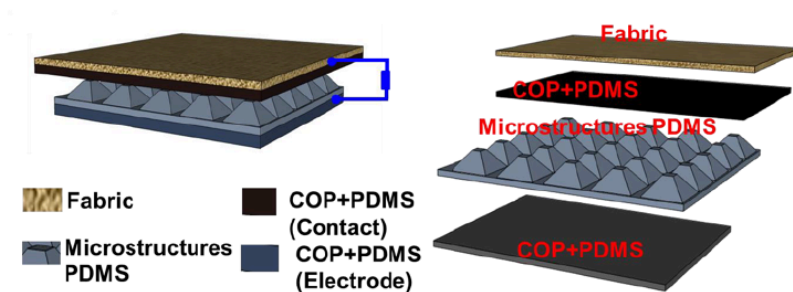


Figure 4: Diagram of the TENG Sensor [2]

Because the TENG sensor can produce up to 40V, we reduce this voltage with a voltage divider so that it does not exceed the maximum voltage input into the ADC. We use 10kΩ and 33kΩ resistors, and the output of this voltage divider is found with the following equation.

$$V_{out} = V_{in} * \frac{10k\Omega}{10k\Omega + 33k\Omega}$$

So, the signal from the sensor from the signal is reduced by a factor of about  $\frac{10}{43}$ . The first entry of Table 2 addresses the third high level requirement, which states that the output voltage of the sensor is reduced by a factor of  $\frac{10}{43} \pm 10\%$ . For a 20V input into the voltage divider, the ideal output would be 4.65V, and the measured voltage is 4.6V, which is a percent error of 1.1%, clearly within 10%.

Following the voltage divider circuit is the unity gain low-current input op-amp. This component was not in our initial design. During testing, we ensured that the ADC worked with the rest of our PCB by inputting random values, but when we input the signal from the TENG sensor, the ADC could not read any values.

Although the sensor produces high voltages, its current output is small and is on the microamps scale. The original circuit incurred a relatively high load onto the sensor, destroying its signal. To address this problem, we added the TL072 op-amp to boost the current. The input bias current of this device is on the order of picoamps, meaning the output signal of the sensor does not get destroyed.

Another design constraint unique to the TENG sensor is its differential output signal. The ADC can only interface with a single-ended input, so the differential signal needed to be converted. We chose the AD8276 difference amplifier for this purpose for its wide input supply range. By powering with the 9V positive supply, and due to its output voltage swing of  $V_s - 0.1.5$ , we were able to attain an output voltage signal of  $\sim 8.5$ .

Table 2: R&V table for the measurement subsystem

Requirement	Verification	Measured Result
Handle up to 40 V differential input and step down to $\sim 10$ V differential.	Using a power supply, generate +20V simulating one end of the sensor and -20V as the other end and probe the output of the voltage divider of both ends, ensuring the difference between the +20V and ground is about 4.65V (9.3V/2).	4.6V

Successfully convert to single-ended signal for ESP32-S3-WROOM-1 compatibility.	Using the multimeter, probe the output of the difference amplifier and the ground reference and ensure the entire signal of ~9.3 is available.	8.7V
---	--	------

## 2.4 Data Processing Subsystem

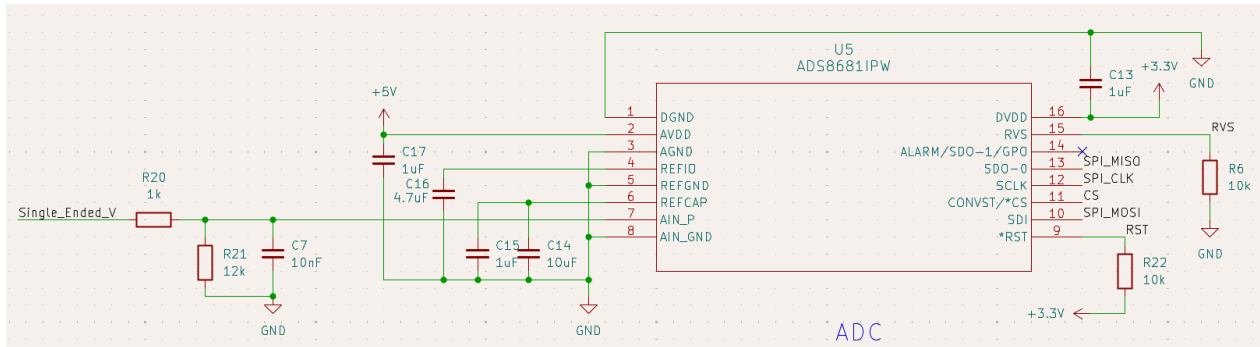


Figure 5: Schematic of the ADC

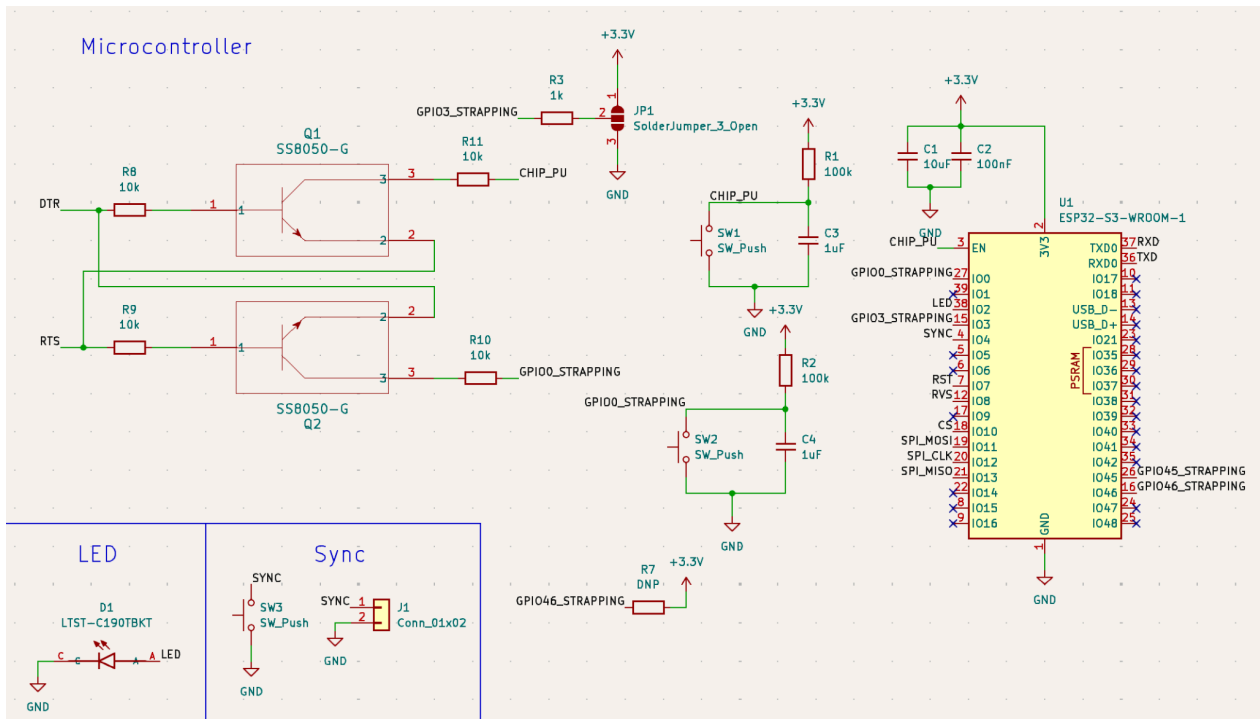


Figure 6: Schematic of the microcontroller, LED, and synchronization button and connector

The data processing subsystem includes the ADS8681 (ADC) and ESP32-S3-WROOM1 (microcontroller), an LED, and a connector and button for synchronization.

The ADS8681 receives the analog signal produced by the measurement subsystem and converts it into a digital signal suitable for the ESP32. It was chosen as a recommendation from Professor Hernandez's lab due to its  $\pm 12\text{ V}$  range and built-in low-pass filter to reduce noise. Additionally it has  $\pm 20\text{ V}$  overvoltage protection to protect against unexpected spikes and 16 bit resolution.

The ESP32-S3-WROOM1 was chosen for its Bluetooth Low Energy (BLE) capability and its dual-core. This component controls other components in the Data Processing Subsystem and transmits and receives data from the mobile application. The functions of the ESP32 are to:

- Maintain a BLE server
  - Notify the mobile app of step timing and magnitude
  - Receive write commands from the mobile app
- Blink status codes on the LED
- Control and read data from the ADC

Due to the importance of data collection and timing. The ADC control was assigned to its own core. The remaining functions were assigned to the other core. The division of functions and communication with the mobile app are shown in Figure 7.

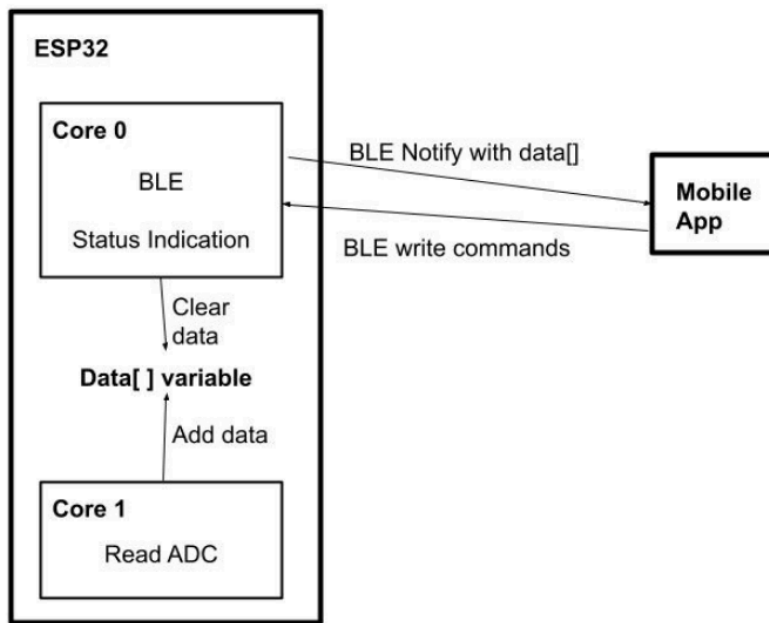


Figure 7: ESP32 + Mobile App Functionality Diagram

In order to save energy and increase efficiency. Effort was taken to minimize the data transmitted over Bluetooth. As such the ADC code implements step detection. If the voltage spikes over a threshold, a step is indicated and its time is recorded. The peak time over the duration of the step is also recorded. This information is stored in an array where time in milliseconds is 4 bytes and the peak voltage is 2 bytes.

For further energy saving, a “low-energy mode” was implemented. The advantage of BLE over classic Bluetooth is its ability to only send data when needed, increasing downtime. To take advantage of this, in “low-energy mode” the esp32 will only send data every 10 seconds as opposed to the default 1 second frequency. The array allotted for sending data is a maximum size of 498 bytes. For upper limit of 5 Hz max step rate, the max data size can be calculated as follows:

$$5\text{Hz} \times 6 \text{ bytes} \times 10 \text{ sec} = 300 \text{ bytes}$$

This is well within the maximum 498 byte limit.

The LED component serves to alert the user of device status. It blinks slowly when turned on and waiting for device connection, and blinks rapidly when waiting for synchronization.

The SYNC component allows the devices to be synchronized almost exactly. When testing Bluetooth synchronization, the latency between the two devices ranged from 8 - 30 milliseconds. This does not adhere to High-Level Requirement 2 of <12 ms. To rectify this, a two wire header connected to ground and a pin on the esp32, and a button between those two rails were added. To synchronize, the devices are connected to each other using a wire and a button on one device is clicked, grounding the corresponding pins on both devices instantaneously. With this change our device adheres to High-Level Requirement 2.

Table 3: R&V table for the data processing subsystem

<b>Requirement</b>	<b>Verification</b>	<b>Measured Result</b>
The ADS8681 is able to properly interface with the microcontroller.	Using a multimeter, probe $V_{ref}$ to ensure it is about 4.096V.	4.092V
The system must transmit 99.9% of data packets over Bluetooth successfully.	Transmitted 200 randomly generated data points.	200/200

*\*The 3.0V provided by the USB-to-UART was insufficient for the ESP32 BLE functionality so it was instead powered directly via power supply (3.3V) or the 3.3V rail on the PCB.*

## 2.5 Programming Subsystem

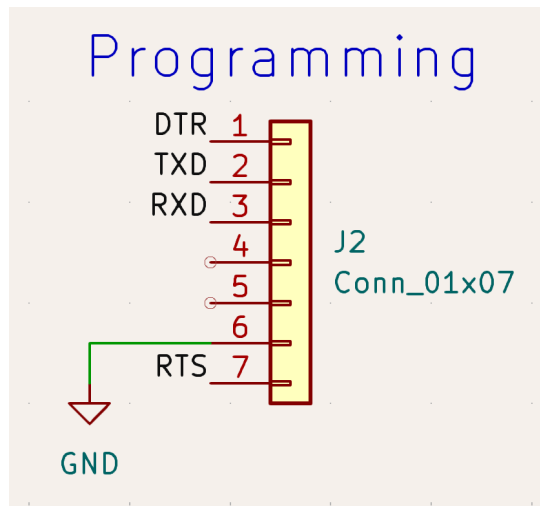


Figure 8: Schematic of the programming subsystem

The programming subsystem allows for programming of the ESP32. It consists of a header for the DTR, TX, RX, RTS, and ground pins on the ESP32. This header connects to a USB-to-UART allowing a computer to program the ESP32 over USB. The USB-to UART is an external device, which allows for the PCB to be as compact as possible as it does not need to be programmed while in use.

Table 4: R&V table for the programming subsystem

Requirement	Verification	Measured Result
The UART transmits and receives data to and from the microcontroller through the TXD and RXD lines, so these pins must be directly connected.	Use a multimeter to check the continuity between the TX pin on the UART and RX pin on the microcontroller and vice versa.	Both passed
The USB-to-UART must provide $3.3 \pm 0.3V$ to the microcontroller.	Use a multimeter to probe the output of the converter and ground to ensure the voltage is within the specified range.	3.0V*

\*The 3.0V provided by the USB-to-UART was insufficient for the ESP32 BLE functionality so it was instead powered directly via power supply (3.3V) or the 3.3V rail on the PCB.

## 2.6 Mobile Application

The purpose of the mobile application is for the user to control the devices and view status from their mobile device. This was implemented in the form of a web application that communicates with the two devices using Bluetooth Low Energy (BLE). Screenshots of the application accompanied with labels and descriptions of the features are shown in Figure 9.

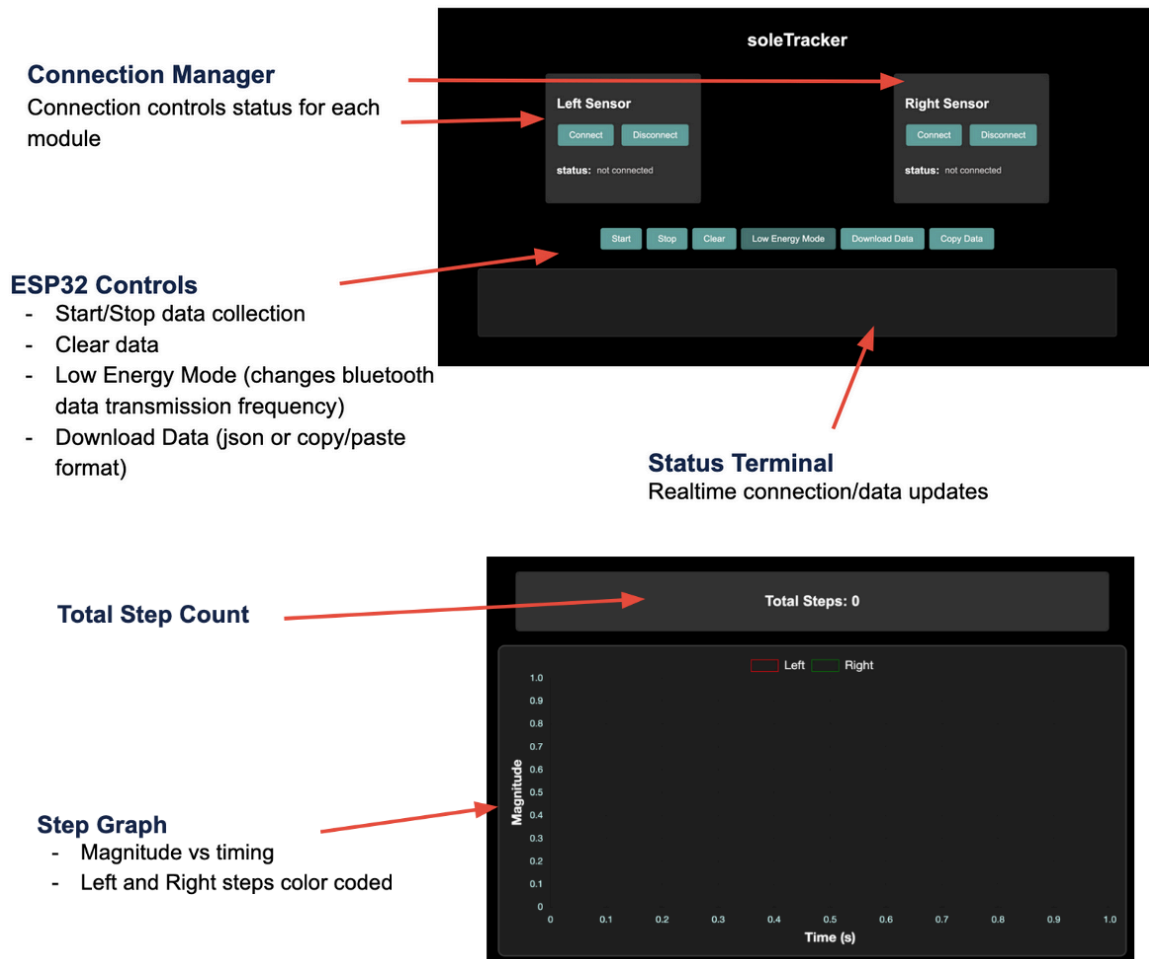


Figure 9: Web Application with Labels and Descriptions

In accordance with High-level Requirement 1, a screenshot of the application with >1000 steps is shown in Figure 10. This also serves as a demonstration of how the application appears when it is populated with data. The left and right foot have approximately the same number of entries\*, indicating both devices are working directly. There are occasional pauses in the data when the user was not walking.

*\*at about 350-450 seconds the right sensor wire detached. To account for the missing data, an extra 289 steps were recorded.*



Figure 10: App Screenshot with 1289 steps.

## 2.7 Mechanical Design

This device is designed to be worn by a user without inhibiting their ability to walk. The sensor is embedded in a custom insole and is wired to the PCB which is housed in a compact enclosure that is strapped to the user's ankle. The overall integration of these components is shown in Figure 11.

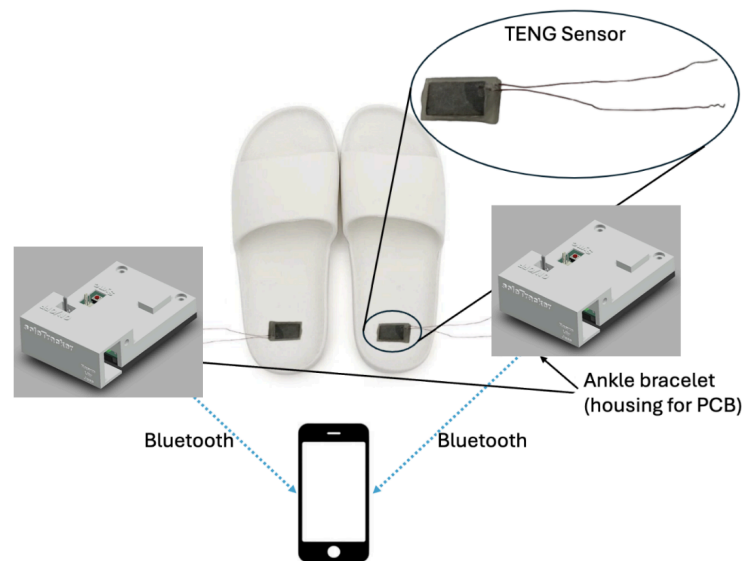


Figure 11: Visual Aid for Overall Design

The custom insole was designed to improve comfort for the user by distributing some of their weight onto the padded insole, while still ensuring the majority of their weight is transferred to the sensor for accurate readings. The enclosure was designed to be as compact and lightweight as possible to reduce footprint, bulkiness, and improve comfort. It has labels for the on/off switch and the SYNC connector and button. It also has a hole for the LED for clear visibility of status indications. The housing comes complete with a hook/loop tape ankle strap for easy attachment to and removal from the user's ankle. The entire assembly is shown in Figure 12.



Figure 12: Final Device Assembly on User

## 3 Cost and Schedule

### 3.1 Costs

1. Labor (\$60/hr)
  - a. Sensor characterization/data collection (10 hours)
  - b. PCB design (20 hours)
  - c. PCB assembly (40 hours)
  - d. Mechanical design (6 hours)
  - e. Mechanical manufacturing (2 hours)
  - f. Software development (40 hours)
2. Parts/Services

With Table 6 in Appendix A, we computed the total cost of all components to be \$84.

Total Cost

- a. Labor:  $118 \text{ hours} * \$60/\text{hr} * 2.5 = \$17,700$
- b. Parts/Services: \$84
- c. Total: \$17,784

## 3.2 Schedule

Table 5: Schedule

Week of 02/02	<ul style="list-style-type: none"> <li>• Initial meeting with Professor Hernandez and sensor testing (Nasym and Jess)</li> </ul>
Week of 02/09	<ul style="list-style-type: none"> <li>• Oscilloscope max voltage testing of sensor (All members)</li> </ul>
Week of 02/16	<ul style="list-style-type: none"> <li>• Development of voltage divider with oscilloscope testing (All members)</li> </ul>
Week of 02/23	<ul style="list-style-type: none"> <li>• Create schematic and PCB (Lily and Jess)</li> </ul>
Week of 03/02	<ul style="list-style-type: none"> <li>• Development of breadboard power system (Lily)</li> <li>• Breadboard wiring of ESP32 with ADC (Jess)</li> <li>• Initial attempt of ADC control with ESP32 (Nasym)</li> </ul>
Week of 03/09	<ul style="list-style-type: none"> <li>• Additional attempt of ADC control with ESP32 (Nasym)</li> <li>• Assembling and testing first PCB design (Lily and Jess)</li> </ul>
Week of 03/16	<ul style="list-style-type: none"> <li>• BLE research and initial code ideation (Nasym)</li> <li>• Modify schematic and update PCB (Lily and Jess)</li> </ul>
Week of 03/23	<ul style="list-style-type: none"> <li>• Further BLE research and testing (Nasym)</li> <li>• Assembling and testing second PCB design (Lily and Jess)</li> </ul>
Week of 03/30	<ul style="list-style-type: none"> <li>• Development of ESP32 BLE server with randomized data and web application (Nasym)</li> <li>• Hardware testing (Lily and Jess)</li> <li>• Updating schematic and PCB (Lily and Jess)</li> </ul>
Week of 04/06	<ul style="list-style-type: none"> <li>• Refinement of BLE server and web app, BLE latency testing (Nasym) <ul style="list-style-type: none"> <li>◦ Ideation of SYNC method for PCB</li> </ul> </li> </ul>
Week of 04/13	<ul style="list-style-type: none"> <li>• Integrating and testing all subsystems (All members)</li> </ul>
Week of 04/20	<ul style="list-style-type: none"> <li>• Development of new ADC code (Nasym)</li> <li>• Debug ESP32 flashing issues (all members)</li> <li>• Enclosure CAD design (Nasym)</li> <li>• Enclosure 3D printing/Assembly (Nasym and Jess)</li> <li>• Development of ankle strap and insole</li> </ul>
Week of 04/27	<ul style="list-style-type: none"> <li>• Addition of buffer breadboard component (Nasym and Jess)</li> <li>• Final testing/debugging/data collection (All members)</li> </ul>
Week of 05/04	<ul style="list-style-type: none"> <li>• Voltage divider refinement and step detection refinement (Nasym and Jess)</li> <li>• Additional verification/testing (All members)</li> </ul>



## 3 Conclusion

Overall, the developed device achieved the overall task of integrating a TENG sensor into a wearable device that transmits step gait data to a user's mobile device. The resulting product is intuitive, accurate, user-friendly, comfortable, and satisfies all prescribed requirements. The device survived over 1000 steps without error, synchronized to within 12 ms and successfully reduced the high-voltage output of the TENG sensor. The team went above and beyond creating both a device and an interfacing application that can be used by all. With clear labels, status indication, and easy setup, the device is clearly intended for its target audience of elderly individuals with health complications.

Although the device met all requirements, there are still some improvements to be made. One future goal of this project is to accurately capture the magnitude of the step, not just the gait. Through preliminary diagnoses, there appears to be clipping somewhere within the processing of the analog signal. In the future resolving this issue would lead to more accurate step magnitude detection. Another improvement would be the overall device quality and comfort. Unfortunately, due to a shortage of 3D printing resources the team was only able to print one iteration of the design. Improvements could be made to the labeling, form factor and manufacturability leading to improved ease of use, comfort, and overall quality for the user. In the future, this device could be embedded into the shoe of the user for reduced setup complexity—allowing the user to simply put on the shoe instead of also having to put on the ankle attachment. A final improvement is to include all the electrical components (apart from the sensor, battery, and USB-to-UART) on the PCB. Due to time constraints, the buffer and its associated circuit had to be added as an external breadboard. This improvement would decrease the size of the device, declutter the wiring, and improve the overall usability.

### 3.1 Safety and Ethics

In developing our gait monitoring system, we prioritize the safety, health, and privacy of the users based on ethical engineering principles. A primary safety concern is the TENG sensor's capability to produce up to 40V under high loads. To ensure user safety, our design has a secure enclosure and adequate wire shielding that prevents exposure to this voltage, mitigating any potential risk. In alignment with the IEEE Code of Ethics Section 1, we have a responsibility to protect the well-being of users and transparently disclose any safety considerations associated with the sensor.

From an ethical standpoint, since our project is developed in collaboration with Professor Hernandez's research group, we properly acknowledge and credit all prior and ongoing contributions, in accordance with ACM Code of Ethics Section 1.5. The sensors used in this project are custom-made and thoroughly documented, so we recognize the efforts of those who designed and developed them. As we continue working alongside Professor Hernandez and his team, we

must ensure that all contributions are fairly attributed. By adhering to these ethical standards, we uphold integrity in our professional activities while ensuring our technology benefits society responsibly.

## 4 Appendix A Costs

Table 6: Parts/Services Costs

Part/Service	Manufacturer/Source	Quantity	Price/Unit	Total Cost	Link
3D printing	SCD/Innovation Studio	~600 grams	~\$0.30/gram	\$18	N/A
M4 bolts	Ace Hardware	4	\$0.60	\$2.40	N/A
M4 nuts	Ace Hardware	4	\$0.30	\$1.20	N/A
5mm High-Density EVA Foam	Hobby Lobby	1	\$7.99	\$7.99	<a href="#">Link</a>
2 Inch Adhesive Black Hook and Loop Tape	GOHOOK	1	\$14.99	\$14.99	<a href="#">Link</a>
ESP32-S3-WR OOM-1	Espressif Systems	1	\$5.49	\$5.49	<a href="#">Link</a>
ADS8681IPW	Texas Instruments	1	\$10.72	\$10.72	<a href="#">Link</a>
AD8276	Analog Devices Inc.	1	\$4.50	\$4.50	<a href="#">Link</a>
282837-2	TE Connectivity AMP Connectors	2	\$0.96	\$1.92	<a href="#">Link</a>
100SP1T1B4 M2QE	E-Switch	1	\$2.97	\$2.97	<a href="#">Link</a>
AZ1117CH2-5 .0TRG1	Diodes Incorporated	1	\$0.56	\$0.56	<a href="#">Link</a>
AZ1117CH2-3 .3TRG1	Diodes Incorporated	1	\$0.56	\$0.56	<a href="#">Link</a>
LT1054CDWR	Texas Instruments	1	\$3.22	\$3.22	<a href="#">Link</a>
LTST-C190TB KT	Lite-On Inc.	1	\$0.25	\$0.25	<a href="#">Link</a>
SS8050-G	Comchip Technology	2	\$0.24	\$0.48	<a href="#">Link</a>
2223-TS04-66 -70-BK-100-S MT-ND	Same Sky (Formerly CUI Devices)	3	\$0.19	\$0.57	<a href="#">Link</a>

(Tactile switch)					
61200621621	Würth Elektronik	1	\$0.43	\$0.43	<a href="#">Link</a>
61300211121	Würth Elektronik	1	\$0.12	\$0.12	<a href="#">Link</a>
TL072CDR	Texas Instruments	1	\$0.28	\$0.28	<a href="#">Link</a>
GRM21BR61 H106ME43L( 10 $\mu$ F Capacitor)	Murata Electronics	7	\$0.26	\$1.82	<a href="#">Link</a>
CL21A226MQ QNNNE (22 $\mu$ F Capacitor)	Samsung Electro-Mechanics	2	\$0.10	\$0.20	<a href="#">Link</a>
CL21A107MQ YNNWE (100 $\mu$ F Capacitor)	Samsung Electro-Mechanics	1	\$0.96	\$0.96	<a href="#">Link</a>
CL21B202KB ANNNC (2000nF Capacitor)	Samsung Electro-Mechanics	1	\$0.10	\$0.10	<a href="#">Link</a>
CC0805KKX5 R9BB225 (2.2 $\mu$ F Capacitor)	YAGEO	1	\$0.25	\$0.25	<a href="#">Link</a>
CL21A475KA QNNNE (4.7 $\mu$ F Capacitor)	Samsung Electro-Mechanics	1	\$0.10	\$0.10	<a href="#">Link</a>
CL21B105KB FNNNG (1 $\mu$ F Capacitor)	Samsung Electro-Mechanics	4	\$0.11	\$0.44	<a href="#">Link</a>
C0805C104K 5RACTU (0.1 $\mu$ F Capacitor)	KEMET	1	\$0.08	\$0.08	<a href="#">Link</a>
C0805C103F5 GECAUTO	KEMET	1	\$1.42	\$1.42	<a href="#">Link</a>

(10nF Capacitor)					
CC0402JRNP 09BN101 (100pF Capacitor)	YAGEO	1	\$0.08	\$0.08	<a href="#">Link</a>
ERA-6AEB20 3V (20k Resistor)	Panasonic Electronic	1	\$0.10	\$0.10	<a href="#">Link</a>
RC0805FR-07 169KL (169k Resistor)	YAGEO	1	\$0.10	\$0.10	<a href="#">Link</a>
RMCF0805JG 10K0 (10k Resistor)	Stackpole Electronics Inc	8	\$0.10	\$0.80	<a href="#">Link</a>
RT0805BRD0 733KL (33k Resistor)	YAGEO	2	\$0.16	\$0.32	<a href="#">Link</a>
RMCF0805JT 1K00 (1k Resistor)	Stackpole Electronics Inc	2	\$0.10	\$0.20	<a href="#">Link</a>
RMCF0805JT 100K (100k Resistor)	Stackpole Electronics Inc	2	\$0.10	\$0.20	<a href="#">Link</a>
ERA-6AEB20 2V (2k Resistor)	Stackpole Electronics Inc	2	\$0.10	\$0.20	<a href="#">Link</a>
RMCF0805JT 12K0 (12k Resistor)	Stackpole Electronics Inc	1	\$0.10	\$0.10	<a href="#">Link</a>

## 5 References

- [1] C. S. Florence, G. Bergen, A. Atherly, E. Burns, J. Stevens, and C. Drake, "Medical Costs of Fatal and Nonfatal Falls in Older Adults," *Journal of the American Geriatrics Society*, vol. 66, no. 4, pp. 693–698, Mar. 2019, doi: <https://doi.org/10.1111/jgs.15304>.
- [2] M. Salauddin, P. Gupta, Y. Fu, M. Hernandez, Y-C. Chang, "Food-Waste Derived Triboelectric Sensors for Biomechanical Monitoring of Frailty Status and Fall Risk in Older Adults," in *Proc. 2025 Design of Medical Devices Conf. (DMD2025)*, Minneapolis, MN, USA, Apr. 2025, pp. 1–4.
- [3] Diodes Incorporated, "Low Dropout Linear Regulator," AZ1117C datasheet, Sep. 2022.
- [4] Texas Instruments, "LT1054 Switched-Capacitor Voltage Converters With Regulators," LT1054 datasheet, Feb. 1990 [Revised July. 2015]
- [5] Analog Devices, "Switched-Capacitor Voltage Converter with Regulator," LT1054/LT1054L datasheet, [Revised Jan. 2020]
- [6] Analog Devices, "Low Power, Wide Supply Range, Low Cost Unity-Gain Difference Amplifiers," AD8276/AD8277 datasheet, May. 2009 [Revised Nov. 2011].
- [7] "Analog to Digital Converter (ADC) - ESP32-S3 - — ESP-IDF Programming Guide v4.4 documentation," Espressif.com, 2016.  
<https://docs.espressif.com/projects/esp-idf/en/v4.4/esp32s3/api-reference/peripherals/adc.html>
- [8] Texas Instruments, "ADS868xW 16-Bit, High-Speed, Single-Supply, SAR ADC Data Acquisition System With Programmable, Bipolar Input Ranges," ADS8681W, ADS8685W, ADS8689W datasheet, Jun. 2024.
- [9] Engineering IT Shared Services, "ECE 445 - Senior Design Laboratory," Illinois.edu, 2025.  
[https://courses.grainger.illinois.edu/ece445/wiki/#/esp32\\_example/index](https://courses.grainger.illinois.edu/ece445/wiki/#/esp32_example/index) Espressif, "ESP32-S3 Series," ESP32-S3 datasheet, Jul. 2021 [Revised Sep. 2024]
- [10] Espressif, "ESP32-S3-WROOM-1 ESP32-S3-WROOM-1U," ESP32-S3-WROOM-1 ESP32-S3-WROOM-1U datasheet, Jul. 2021 [Revised Nov. 2024].
- [11] "ESP32 Technical Reference Manual," Espressif Systems, 2025. Accessed: Mar. 06, 2025. [Online]. Available: [https://www.espressif.com/sites/default/files/documentation/esp32\\_technical\\_reference\\_manual\\_en.pdf](https://www.espressif.com/sites/default/files/documentation/esp32_technical_reference_manual_en.pdf)
- [12] IEEE, "IEEE Code of Ethics," [ieee.org](http://www.ieee.org), Jun. 2020.  
<https://www.ieee.org/about/corporate/governance/p7-8.html>
- [13] Association for Computing Machinery, "ACM code of ethics and professional conduct,"

Association for Computing Machinery, 2018. <https://www.acm.org/code-of-ethics>